Preliminary Evaluation of Ground Motions from Earthquakes in Alberta

by Mark Novakovic and Gail M. Atkinson

INTRODUCTION

Between 9 September 2013 and 22 January 2015, more than 900 seismic events in local magnitude (M_L) range 1–4 were detected and located in near-real time by the new TransAlta/Nanometrics network in western Alberta, which commenced operation in the fall of 2013. The network comprises 27 three-component broadband seismograph stations, located as shown in Figure 1, which act in cooperation with other real-time seismograph stations operated by the Alberta Geological Survey (AGS) (Stern *et al.*, 2011) and the Geological Survey of Canada (GSC). There are additional campaign-mode stations in the Canadian Rockies and Alberta Network (CRANE) network operated by the University of Alberta (Gu *et al.*, 2011).

In this study, we compile and analyze a ground-motion database of 5% damped pseudospectral acceleration (PSA) from the signals recorded on the TransAlta/Nanometrics stations in order to gain an initial understanding of overall ground-motion source, attenuation, and site characteristics in the region. A catalog of events is provided on www.inducedseismicity.ca (last accessed May 2015); the locations and initial magnitudes of events were obtained by Nanometrics (www.nanometrics.ca; last accessed May 2015). We processed the recorded time series as described in Assatourians and Atkinson (2010). Briefly, the velocity time series are corrected for glitches and trends, then filtered and corrected for instrument response in the frequency domain. Differentiation to generate acceleration time series is done in the frequency domain before conversion back to the time domain. Horizontal and vertical peak ground velocity and peak ground acceleration values are computed from peak amplitudes of instrument-corrected time series, and 5% damped PSAs are calculated from the corrected acceleration time series following the Nigam and Jennings (1969) formulation for the computation of response spectra. The results of the processing procedures were validated against other standard processing software, as described in Assatourians and Atkinson (2010).

The TransAlta/Nanometrics data will be supplemented in the future with recordings from the AGS, GSC, and CRANE networks, but these networks require significant additional compilation and processing effort to obtain reliable ground-motion amplitudes. In particular, we encountered quality-control issues in the instrument response information in some cases, which has made it difficult to utilize all stations from all networks. In our initial evaluation, we therefore focus on the high-quality Standard for Exchange of Earthquake Data (SEED) datafiles provided by the TransAlta/Nanometrics network, which can be most readily analyzed.

An issue encountered in the database compilation is that many of the seismic events listed in the catalog are suspected to be blasts from mining or quarry operations, which are difficult to distinguish automatically from earthquakes (either natural or induced) in near-real-time operations. A manual review of waveforms from all events across the province is beyond the scope or resources of the analysis team (such reviews are conducted only for events in areas of particular client interest). For this study, we are relying on a blast discrimination technique developed by Fereidoni and Atkinson (2015), which is based on the ratio of the vertical-component PSA over the horizontal-component PSA at a frequency of 10 Hz ($PSA_H[10]/PSA_V[10]$). Fereidoni and Atkinson (2015) showed that ($PSA_H[10]/PSA_V[10]$) is much greater for blasts than for earthquakes for observations recorded within 100 km of the event. This technique is only applicable for some of the areas of our database, because it requires the existence of stations within 100 km. Our discrimination of blasts, as shown in Figure 1, is thus preliminary. For example, we suspect that many of the events in the area near Jasper National Park are also blasts, but we are not yet able to automatically distinguish blasts from earthquakes in this region. Therefore, we retained the earthquake designation for these events at present.

Another important issue in the database evaluation that is not yet resolved is the discrimination of natural events from those that are suspected to be induced. Approximately 80% of the events in our database occur in distinct clusters in time and space that are characteristic of induced events. On the basis of other studies, the locations of most of these clusters coincide with areas suspected to be induced-seismicity sources. For example, the events in the Crooked Lake region are strongly related in both time and space to hydraulic fracturing in horizontal wells in the Duvernay formation (Schultz *et al.*, 2015). Events in the Brazeau River region (south of Crooked Lake and west of Edmonton) are strongly correlated with activities at a disposal well in the area (Schultz *et al.*, 2014), whereas events in the Rocky Mountain House area (west of Red Deer) have been related to gas extraction activities (Baranova *et al.*, 1999). In this study, we do not attempt to distinguish natural from induced seismicity on an event-by-event basis, as this would be beyond the present scope. However, as noted above, due to the location and timing of events we believe that the great majority of them (~80%) are potentially induced.

doi: 10.1785/0220150059

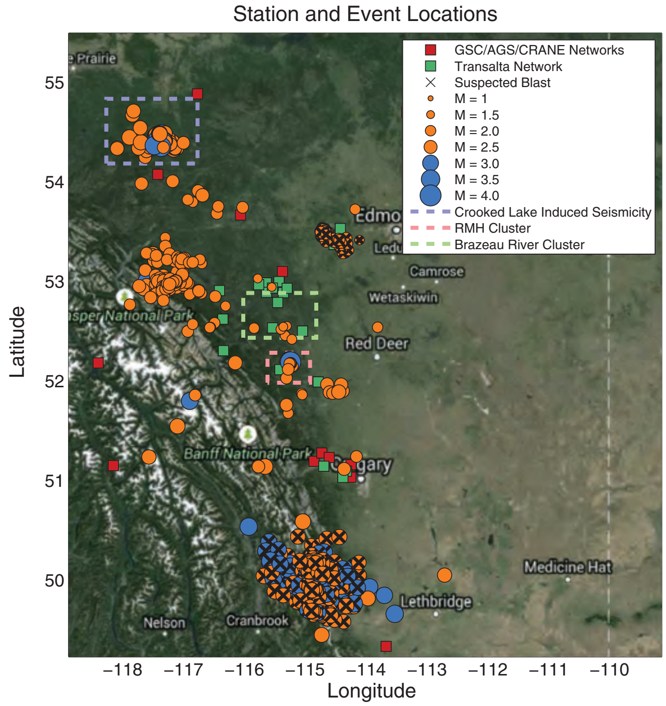

▲ **Figure 1.** Locations of stations and study events in Alberta. Events that are considered to be blasts are designated by an x within the magnitude symbol. Note that the deformation front that marks the boundary of the Rocky Mountains is distinguishable by topography.

MAGNITUDE EVALUATIONS

For each event in the database, we estimated the moment magnitude ($\mathbf{M}$) using the PSA-based algorithm of Atkinson *et al.* (2014, hereafter denoted as AGY14):

$$\mathbf{M} = \{\log_{10}(\mathrm{PSA}_T) - C_T + \log_{10}[Z(R)] + \gamma_T R\}/1.45, \quad (1)$$

in which R is the hypocentral distance and

$$Z(R) = 1.3\log_{10}(R) \quad \text{for } R \le 50 \text{ km} \quad (2a)$$

and

$$Z(R) = 1.3\log_{10}(20) + 0.5\log_{10}(R/50) \quad \text{for } R > 50 \text{ km}. \quad (2b)$$

PSA_T is the PSA value of the vertical component at period T, C_T is an empirical calibration term, γ_T is the anelastic attenuation term at period T, and $Z(R)$ is a geometric spreading model. As recommended by AGY14 model, we set the focal depth (h) to 5 km to enable a rapid and robust determination of R, even if the depth is not well known. The computed value of R is not sensitive to h, with the exception of the rare observations that are made very close to the source. Our preliminary evaluation of attenuation (as shown later in this article) suggests that the western North American (WNA) crustal attenuation model is appropriate for the study events in this region, regardless of whether the events are east or west of the deformation front that marks the edge of the Rocky Mountains (visible in Fig. 1). For WNA, AGY14 model gives recommended values for γ_T and C_T as noted in Table 1, which we adopt for use in magnitude determination.

Table 1
Western North American (WNA) Anelastic Attenuation (γ_T) and Empirical Calibration (γ_T) Terms for 1.00 Hz and 3.33 Hz Frequencies

	WNA 1.00 Hz	WNA 3.33 Hz
C_T	4.25	3.15
γ_T	0.0035	0.004

We use equation (1) to calculate $\mathbf{M}$ for each observation, based on the observed PSA_V and R. AGY14 model suggests that $\mathbf{M}$ be calculated from the 1 Hz PSA in general but that for events of $\mathbf{M} < 3$ it is preferable to use the 3.33 Hz PSA due to noise issues that inflate the 1 Hz amplitudes. A question then arises as to which ground-motion measure to use for events that are close to $\mathbf{M}$ 3, because slightly different values will result based upon this choice. Moreover, the estimated value will also depend somewhat on the distance constraints applied, because noise issues become more problematic for more distant stations. Based on our preliminary evaluation of the ground-motion data and its attenuation and noise behavior with distance, we restricted the distance range of stations used in magnitude determination as follows: we use all stations with $R < 150$ km for events of $\mathbf{M} \le 2.6$ and all stations with $R < 300$ km for events with $\mathbf{M} > 2.6$. As a quality-control measure, we exclude any station for which the value of $\mathbf{M}$ exceeds $\pm 2\sigma$ of the event average, in which σ is the standard deviation. The average $\mathbf{M}$ for each event is recalculated after this initial screening, using both the 1.00 and 3.33 Hz definitions (denoted $\mathbf{M}$(1 Hz) and $\mathbf{M}$(3.33 Hz)). The final $\mathbf{M}$ assigned to an event is determined based on the following criteria:

1. if $\mathbf{M}(1\text{ Hz}) < 3$ and $\mathbf{M}(3.33\text{ Hz}) < 3$, then $\mathbf{M} = \mathbf{M}(3.33\text{ Hz})$; or
2. if $\mathbf{M}(1\text{ Hz}) \ge 3$ and $\mathbf{M}(3.33\text{ Hz}) \ge 3$, then $\mathbf{M} = \mathbf{M}(1\text{ Hz})$; otherwise
3. $\mathbf{M} = [\mathbf{M}(1\text{ Hz}) + \mathbf{M}(3.33\text{ Hz})]/2$.

In other words, we use the 3.33 Hz measure if $\mathbf{M}$ is clearly below 3, the 1 Hz measure if $\mathbf{M}$ is clearly above 3, or an average of the two if the measures are ambiguous.

The estimated value of $\mathbf{M}$ is plotted against the local magnitude (M_L) values, as computed by Nanometrics, in Figure 2. In general, the calculated value of $\mathbf{M}$ tracks the 1 : 1 line against M_L well for events of $\mathbf{M} > 2.6$; for such events, the average value of $\mathbf{M} - M_L = 0.17 \pm 0.06$. There is a cluster of events of high M_L relative to the overall trend. The M_L of these events may tend to be overestimated because they occurred in the Fox Creek area where the network coverage of the TransAlta/Nanometrics network is poor. The inclusion of

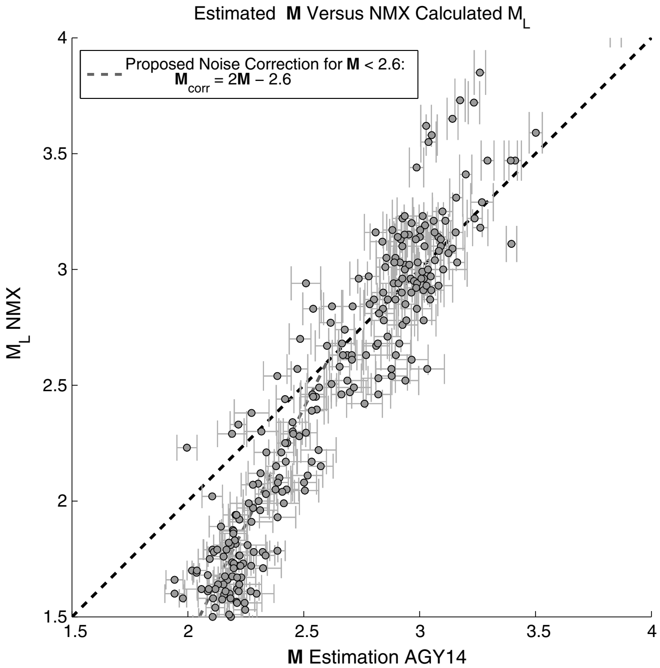

▲ **Figure 2.** Estimated **M** versus M_L (excluding events designated as blasts). Standard error of **M** estimates are also shown (horizontal bars, with verticals to denote edges).

distant noisy stations may have biased the magnitude estimates for these events. The low-magnitude range on Figure 2 is also affected by noise issues, as indicated by the departure of the M_L versus **M** trend from the 1:1 line. For very weak motions, the response of an oscillator is driven by low-frequency noise, even at higher frequencies. The ideal solution would be to have quieter sites, but this would require expensive borehole installations. A more practical alternative (at least in the short term) is to devise an appropriate correction for the noise to reduce the bias in the determined values of **M**. By inspection of Figure 2, we suggest that such a correction for the stations of the TransAlta/Nanometrics network in western Alberta is given by the line

$$\mathbf{M}_{corr} = 2\mathbf{M} - 2.6 \quad \text{for } \mathbf{M} < 2.6, \tag{3}$$

in which $\mathbf{M}_{corr}$ is the noise-corrected estimate of the moment magnitude, based on the computed value of **M**.

EVALUATION OF GROUND MOTIONS

Figure 3 shows the distribution of events in magnitude and distance space, after correction of the **M** value for noise as indicated in equation (3). Ground motions have been compiled into a database. The PSA values from the vertical and horizontal components for sample frequencies between 0.2 and 50 Hz are compiled along with metadata. The metadata include the date, time, event location, station location, hypocentral distance, estimated **M**, other computed magnitudes such as M_L (where available), and focal depth (where known).

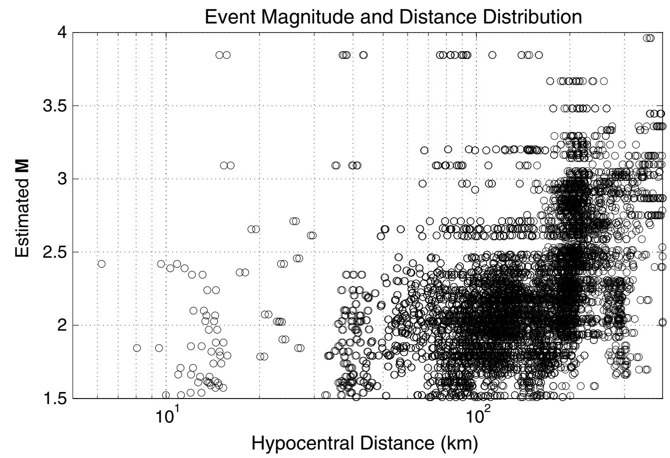

▲ **Figure 3.** Distribution of events (blasts excluded) in **M** and distance.

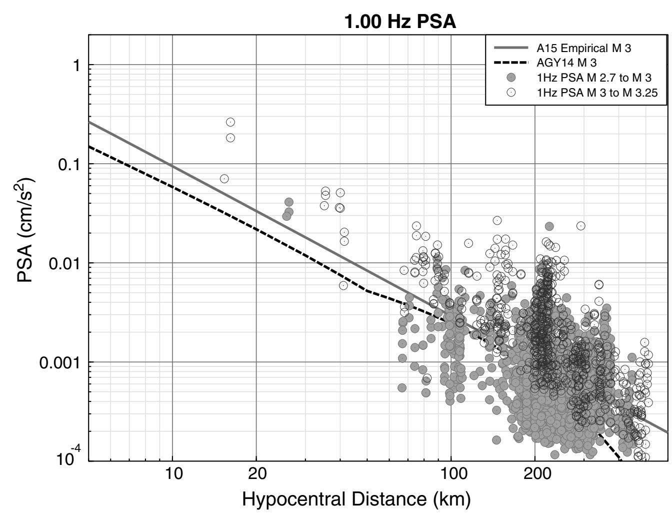

▲ **Figure 4.** Pseudospectral acceleration (PSA) amplitudes (all components) at 1 Hz for events of $\mathbf{M} = 3.0 \pm 0.3$, as a function of hypocentral distance, compared to the relations of Atkinson *et al.* (2014; denoted as AGY14; vertical component) and Atkinson (2015; denoted as A15; horizontal component, B/C conditions).

In Figures 4 and 5, we provide an initial overview of the motions and their attenuation at 1 and 3.33 Hz for events of $\mathbf{M} \sim 3$. We compare the observed amplitudes to (1) the WNA equation of AGY14 model used to define **M** and (2) the ground-motion prediction equation (GMPE) of Atkinson (2015, hereafter denoted as A15) developed for small-to-moderate events. The A15 GMPE was developed from PSA data in a similar magnitude range in California. The AGY14 equation is for the vertical component (assumed to have negligible site response), whereas the A15 equation is for the geometric mean of the horizontal components, for National Earthquake Hazards Reduction Program (NEHRP; Building Seismic Safety Council, 2009) class B/C site conditions (near-surface shear-wave velocity of 760 m/s); all three observed components are plotted. Overall,

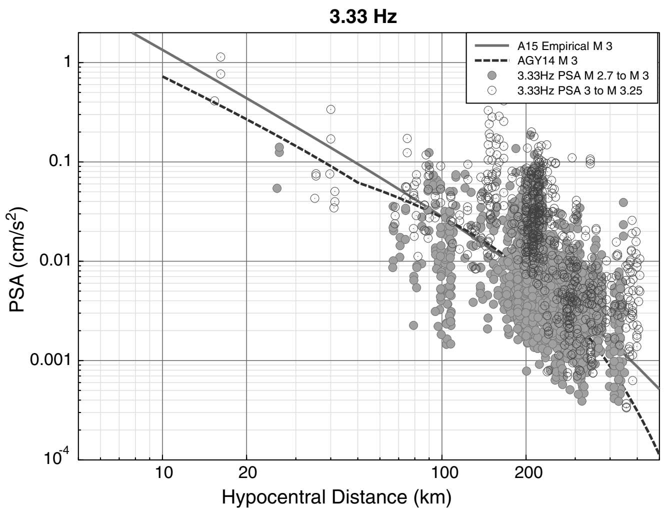

▲ **Figure 5.** The PSA amplitudes (all components) at 3.33 Hz for events of $\mathbf{M} = 3.0 \pm 0.3$, as a function of hypocentral distance, compared to the relations of AGY14 (vertical component) and A15 (horizontal component, B/C conditions).

the motions are in qualitative agreement with the expected amplitude and attenuation trends, suggesting that overall the western attenuation model is a reasonable first approximation. This is perhaps surprising, as we might have expected a mixture of eastern and western attenuation types in this region because it is so close to the deformation front. It could be that crustal complexity extends several hundred kilometers east of the deformation front, such that the entire region is more nearly a western than eastern tectonic setting. We examine our first impressions in more detail in the following.

To gain insight into the attenuation and magnitude-scaling features of the ground-motion data, it is useful to evaluate the residuals relative to a reference prediction equation (where the residual for an observation is defined as $\log(\mathrm{PSA_{obs}}) - \log(\mathrm{PSA_{pred}})$). Trends in the differences between observations and predictions plotted versus distance allow us to refine our model of attenuation with distance, whereas trends in magnitude are informative regarding source scaling. A constant offset may reflect a combination of effects including differences in source level (i.e., stress parameter) and site amplification. For the predicted values, we use the A15 small-**M** empirical GMPE developed for California, including the recommended additional c_4 term to extend the GMPE to regional distances. Thus the reference prediction GMPE is given by

$$\log_{10} \mathrm{PSA} = c_0 + c_1\mathbf{M} + c_2\mathbf{M}^2 + c_3 \log R_{\mathrm{eff}} + c_4 R_{\mathrm{eff}} \tag{4}$$

(Atkinson, 2015), in which R_{eff} is an effective point-source distance that includes near-source distance-saturation effects using an effective depth parameter

$$R_{\mathrm{eff}} = \sqrt{(R^2 + h_{\mathrm{eff}}^2)} \tag{5}$$

(Yenier and Atkinson, 2014). Here, R is the hypocentral distance and

$$h_{\mathrm{eff}} = \max(1, 10^{(-1.72+0.43\mathbf{M})}). \tag{6}$$

A minimum value of $h_{\mathrm{eff}} = 1$ km is specified; this is the value taken by equation (6) when $\mathbf{M} = 4$.

Figure 6 plots the PSA residuals with respect to the A15 model, in which the event magnitude is as calculated by the AGY14 **M** estimation model described above. To focus on the higher-quality data, we consider only events of $\mathbf{M} \geq 2.6$. The site conditions of the sites are not well known and are currently under investigation. However, all sites have posthole seismometers driven into the surficial soil layer. The instruments are thus founded at the level of resistance for a posthole auger. It is possible that this results in a relatively common site condition among stations, if the regional near-surface geology is not highly variable in nature. If so, it would be a significant benefit to this installation method. In this study, we do not attempt to subtract site effects from the observations, as they are so poorly known. Rather, we use the comparisons between observations and prediction equations to infer what site response terms might account for the observed residuals then evaluate whether these are reasonable. For example, the residuals for the vertical-component observations with respect to the A15 GMPE might be expected to be minimal, under the assumption that the vertical component is a proxy for the unamplified horizontal-component motions (e.g., Lermo and Chávez-García, 1993; Ghofrani and Atkinson, 2014). In contrast, we might expect significant positive residuals for the horizontal components because the instruments are located within the soil layer (not on firmer B/C site conditions).

What we see in Figure 6 is generally consistent with those expectations, with some exceptions. Overall, there is no compelling evidence for significant deviations of the attenuation model from the trends given in the A15 model. However, there are some deviations from a flat trend in the attenuation residuals. Specifically the 3.33 Hz vertical-component PSA values have near-zero average residuals with respect to the A15 model at $R > 150$ km but have negative residuals at closer distances. In contrast, at 1 Hz the vertical-component residuals are near zero at $R < 150$ km but negative at larger distances. The 1 Hz horizontal PSA residuals are generally positive, suggesting significant site amplification; the 3.33 Hz horizontal PSA residuals are also largely positive but more ambiguous at closer distances. At 10 Hz, the residuals are negative at $R < 150$ km on both components but positive on both components at $R > 150$ km. This suggests that there may be significant effects of noise on the spectral response and/or that a more complex attenuation model may be warranted (perhaps a bilinear model with a change in geometric spreading at $R < 100$ km). These overall trends are shown more clearly in Figure 7, which plots the mean and standard error of the residual data of Figure 6 binned in distance bins 0.2 log units in width. Because of the paucity of near-distance data, the only truly compelling trends are the positive residuals at $R > 150$ km on the horizontal component at 3.33 Hz, and on

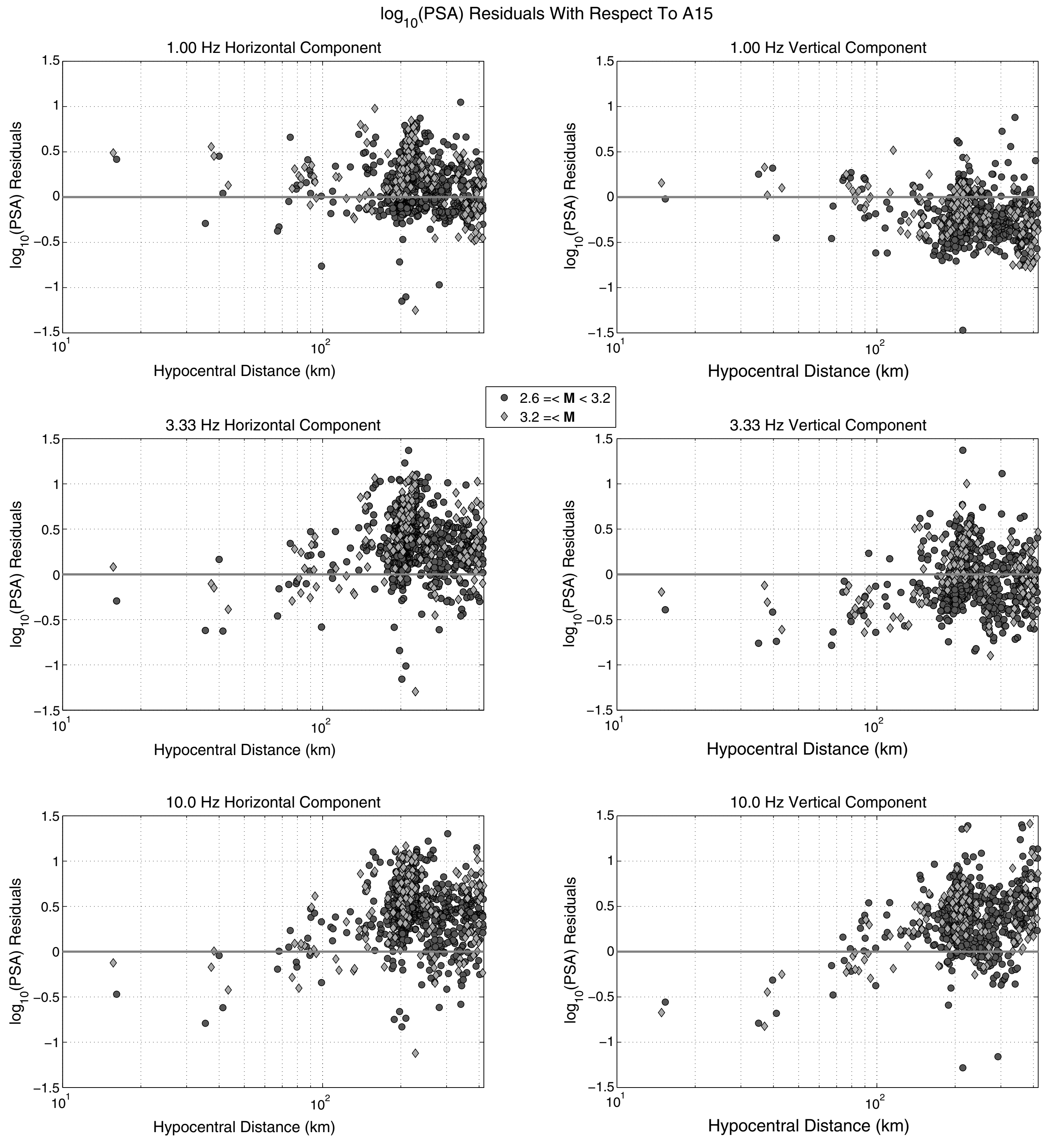

▲ **Figure 6.** The PSA residuals for **M** ≥2.6 for PSA at (top) 1.00 Hz, (middle) 3.33 Hz, and (bottom) 10 Hz for (left) horizontal and (right) vertical components. (Blasts have been removed.)

both components at 10 Hz. The attenuation model will be refined because more observations at close distances are obtained, enabling the trends to be more accurately defined.

If we subtract the terms in c_3 and c_4 of equation (4) from the observed PSA for each station, we can determine average source terms for each event; these are the amplitudes that would be observed at near-source distances. Figure 8 plots these source terms relative to the empirical A15 model. The expected magnitude scaling based on the point-source simulation model of Yenier and Atkinson (2015a) for California is also shown

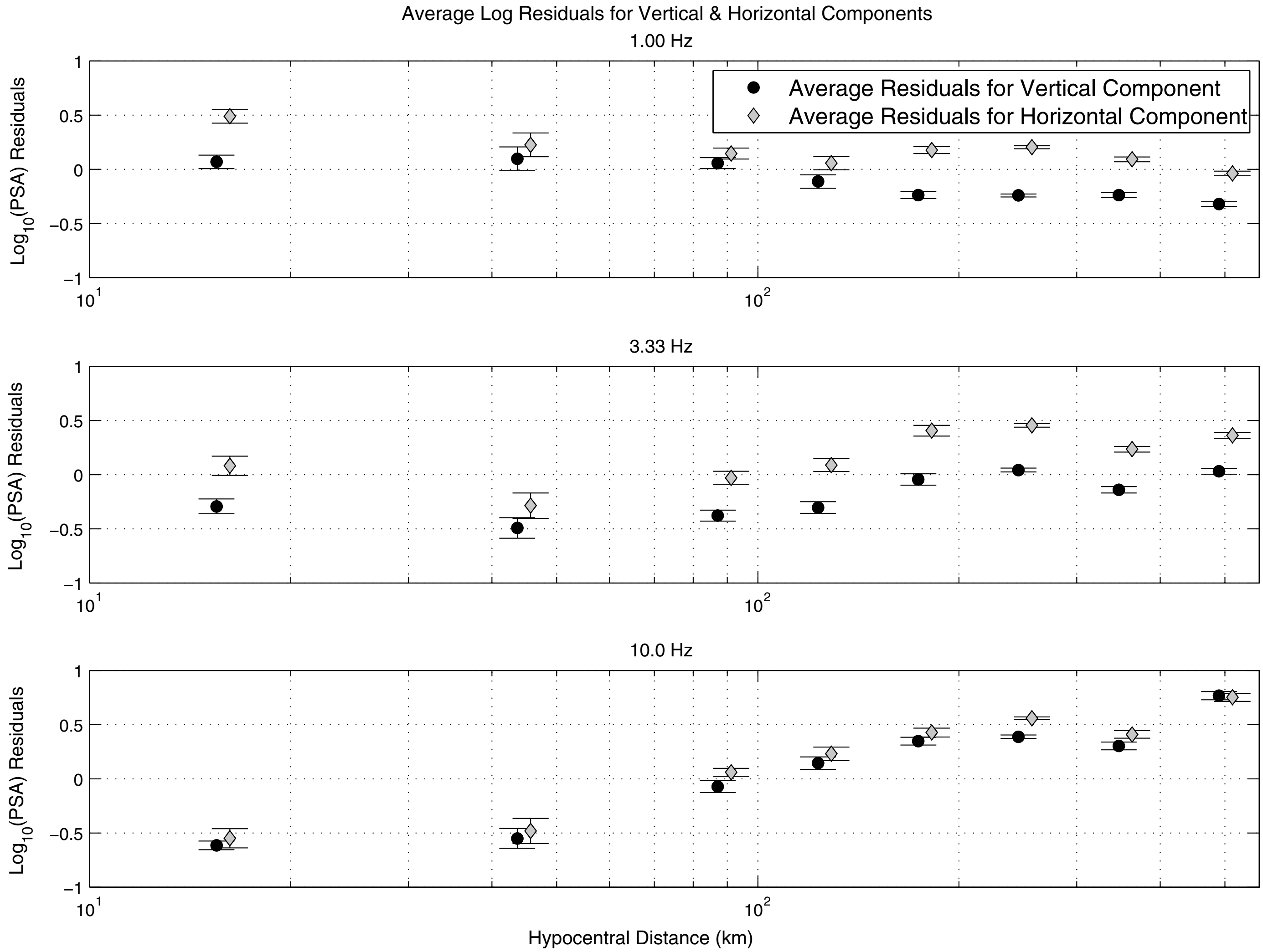

▲ **Figure 7.** The mean and standard error of PSA residuals for **M** ≥2.6 at (top) 1.00 Hz, (middle) 3.33 Hz, and (bottom) 10 Hz, binned in log distance bins, for horizontal and vertical components. No error bar is plotted if the number of observations in the bin is <3. A slight offset from the bin center is used for plotting clarity (to distinguish horizontal from vertical).

(shifted by the appropriate calibration constant so that it matches the level of the A15 model in the **M** 3–6 range, where both are applicable); this model provides the expected scaling for a Brune source model with a stress parameter of 100 bars. It is important to recognize that both the Yenier and Atkinson (2015a) and Atkinson (2015) scaling were defined for events of **M** >3, and thus both represent significant extrapolations to lower magnitudes on Figure 8. At **M** >3, the empirical and point-source scalings are very close to each other, whereas the extrapolated scaling at lower magnitudes shows some deviation between the two models. Overall, the magnitude scaling of the source terms is very similar to that expected for a 100-bar point-source model. It should be acknowledged that for the 1 Hz scaling, it is expected that it should follow the point-source scaling of Yenier and Atkinson (2015a) for events of **M** >3 (because the event magnitudes have been determined from a similar point-source model), and thus there is some circularity. However, the scaling in the A15 model is entirely empirical as derived from a different database (the Next Generation Attenuation [NGA]-West 2 database; Pacific Earthquake Engineering Research Center, 2014). Moreover, as frequency increases, the scaling will not be controlled by the estimated moment magnitude, but instead becomes more dependent on the stress parameter. At 10.0 Hz, the attenuation-corrected ground motions are significantly higher than predicted. However, because of the attenuation trends noted at $R < 150$ km (Figs. 6 and 7), it would be premature to draw conclusions regarding the overall stress parameter from this observation. The scaling behavior with magnitude requires further investigation after sufficient data to define the attenuation at closer distances are obtained, allowing more robust source characterization.

In considering the source characteristics of the events, it should be noted that at frequencies of 1 Hz and lower, PSA amplitudes are insensitive to stress parameter in the magnitude range covered in this study. However, stress parameter becomes important with increasing frequency, which is at least part of

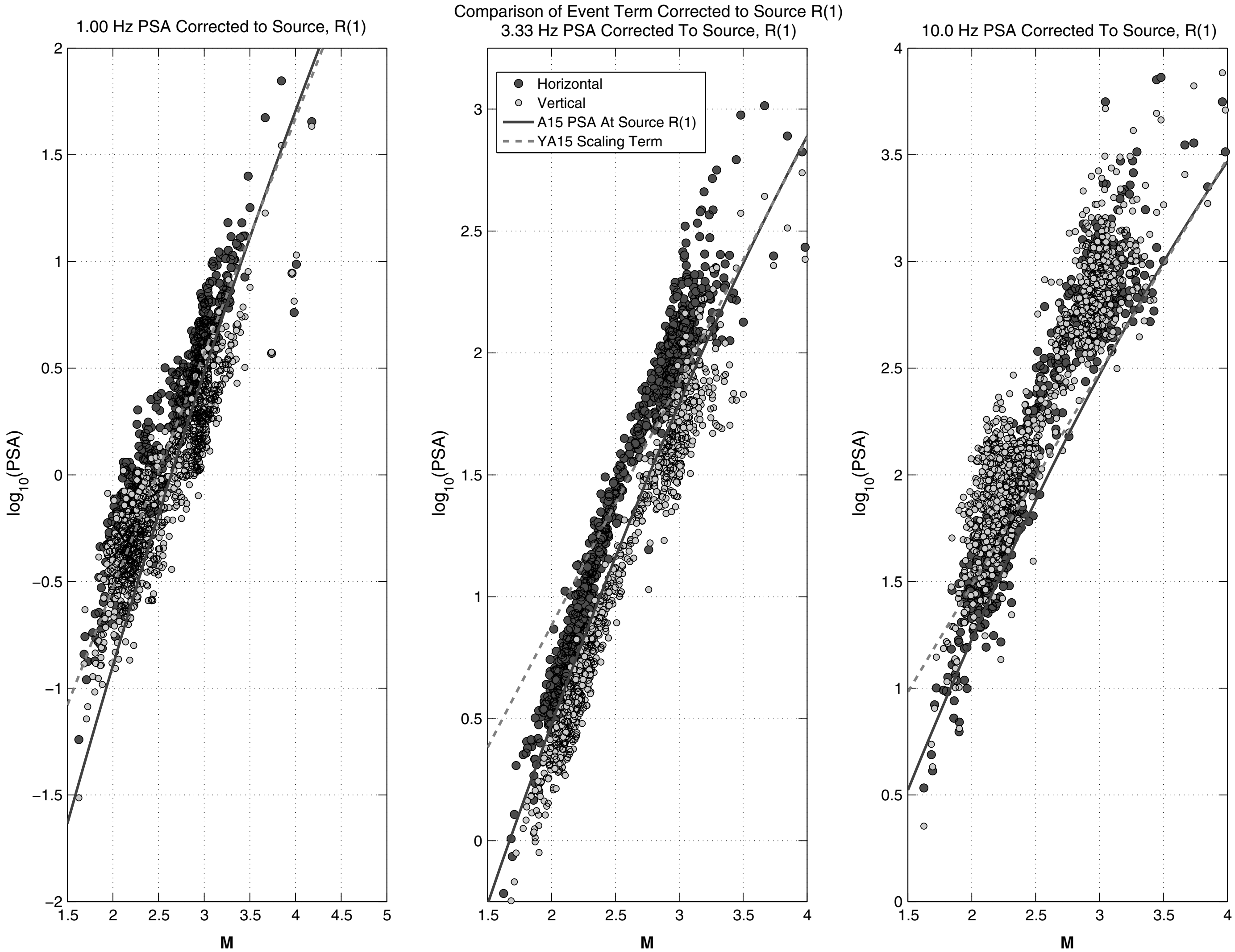

▲ **Figure 8.** Scaling of source terms with magnitude, in comparison to empirical (A15) and simulation-based (Yenier and Atkinson, 2015a) models.

the reason why the scatter is broader at 10 Hz than at 1 Hz in Figure 8. It has been suggested that stress parameter may be smaller for induced events than for natural events, leading to weaker ground motions (Hough, 2014). This may be primarily a focal depth effect, because Yenier and Atkinson (2015a,b) showed that stress parameter increases with focal depth in both WNA and central and eastern North America (CENA). Specifically, Yenier and Atkinson (2015a,b) found that average stress parameters for shallow events (<5 km) of **M** 3–5 are about 10 bars on average for WNA and about 30 bars on average for CENA, although there is much interevent variability (by a factor greater than 2). For events with depths of 10 km or greater, the average stress parameters are about 10 times higher than those for very shallow events, in both regions. Thus the focal depth effect on stress parameter may overwhelm any differences due to an eastern or western tectonic setting. Furthermore, it may be difficult to distinguish between focal depth effects and event-type effects (natural versus induced) on stress parameter. Further study with events covering a broader distance range will be required to determine the average stress parameters in this region and to resolve the influence that competing factors may have upon the stress parameter of events.

In Figure 9, we examine the average residual versus frequency in selected distance ranges, for frequencies of 0.5 Hz and greater (noise issues are too severe at lower frequencies). We can interpret Figure 9 as an average site response curve for the stations, relative to the reference B/C condition of Atkinson (2015). However it should be acknowledged that this term also includes any net bias, whether or not it is attributable to site conditions or other factors such as overall source effects, noise issues, and so on. Specifically, it is likely that the large positive term at $f < 1$ Hz and $f > 10$ Hz is largely driven by noise. In particular, at $f < 1$ Hz the PSA is largely attributable to the oscillator response to the prominent 0.3 Hz microseismic noise peak. Noise may also be responsible for the distance dependence of the average residual term, because

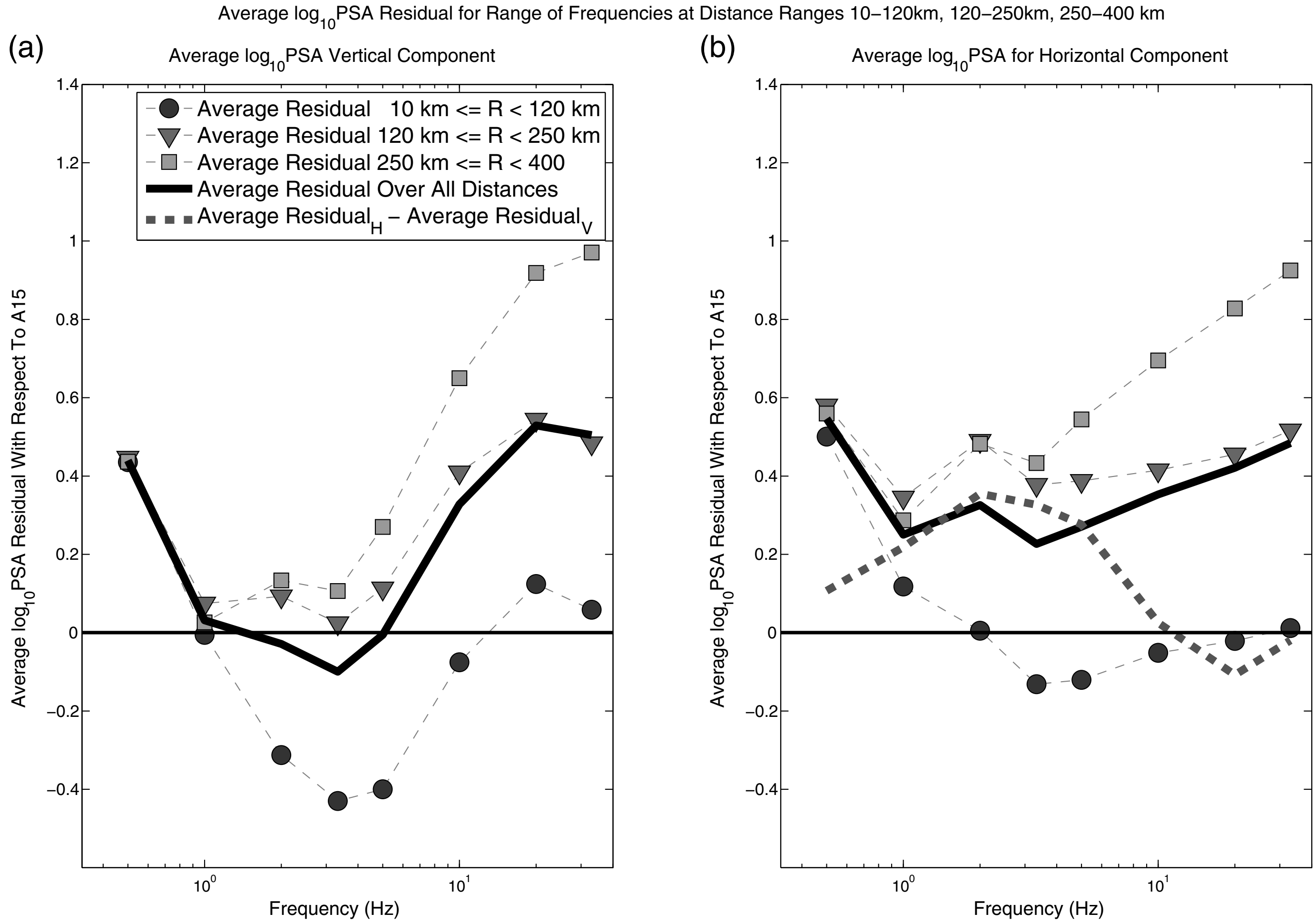

▲ **Figure 9.** The average PSA residuals versus frequency in distance ranges 10–120 km, 120–250 km, 250–400 km for (a) vertical and (b) horizontal components. The average, including all distances, is also shown (heavy line). The dashed line in (b) shows the average horizontal residual minus the average vertical residual, which is similar to an average site response function.

it has a relatively larger contribution to amplitudes for the weak motions observed on distant stations. Overall, it appears that the site response is about 0.2 log units greater on the horizontal than the vertical component (factor of 1.6). Moreover, there is a noticeable peak in the horizontal response curve at a frequency near 2 Hz that is not present on the vertical component. Finally, the trend to larger amplitudes at high frequencies relative to the predictions of Atkinson (2015) could reflect a combination of noise and/or lesser near-surface attenuation (e.g., smaller value of the kappa parameter of Anderson and Hough, 1984) relative to California sites.

To remove the influence of noise on the overall site response term in Figure 9, which should be common on the vertical and horizontal components, we subtract the average vertical-component response curve from the average horizontal-component response curve. The resulting line (Fig. 9b) is similar to an average horizontal-to-vertical (H/V) ratio plot over all records. It suggests that the dominant feature of the response of these sites is a peak in the frequency range from 2 to 5 Hz. This is in agreement with the preliminary results of H/V studies for sites in the region (Farrugia and Atkinson, 2015). The H/V ratio is a well-known method for estimating the total amount of amplification a site will experience during a seismic event and in particular for determining the fundamental frequency at that site (Lermo and Chávez-García, 1993; Ghofrani and Atkinson, 2014). Preliminary H/V studies (Farrugia and Atkinson, 2015) suggest that the TransAlta network stations all have very similar site responses, with a pronounced amplification in the 2–5 Hz frequency band on most stations that is consistent with expectations for relatively shallow soft-soil sites underlain by hard rock.

If we interpret the residuals as site-response terms, we can infer the amplification relative to the A15 reference condition of B/C by computing the average residual at each station. As shown in Figure 10, the inferred site terms are relatively consistent from one station to the next (consistent with the results of Farrugia and Atkinson, 2015). This suggests that an overall typical site amplification curve, as given in Figure 9 (dashed line), may be a reasonable way to model site effects at the stations.

As more ground-motion observations are collected, we will be able to further resolve the competing influences of source, attenuation, and site factors on the observed ground motions

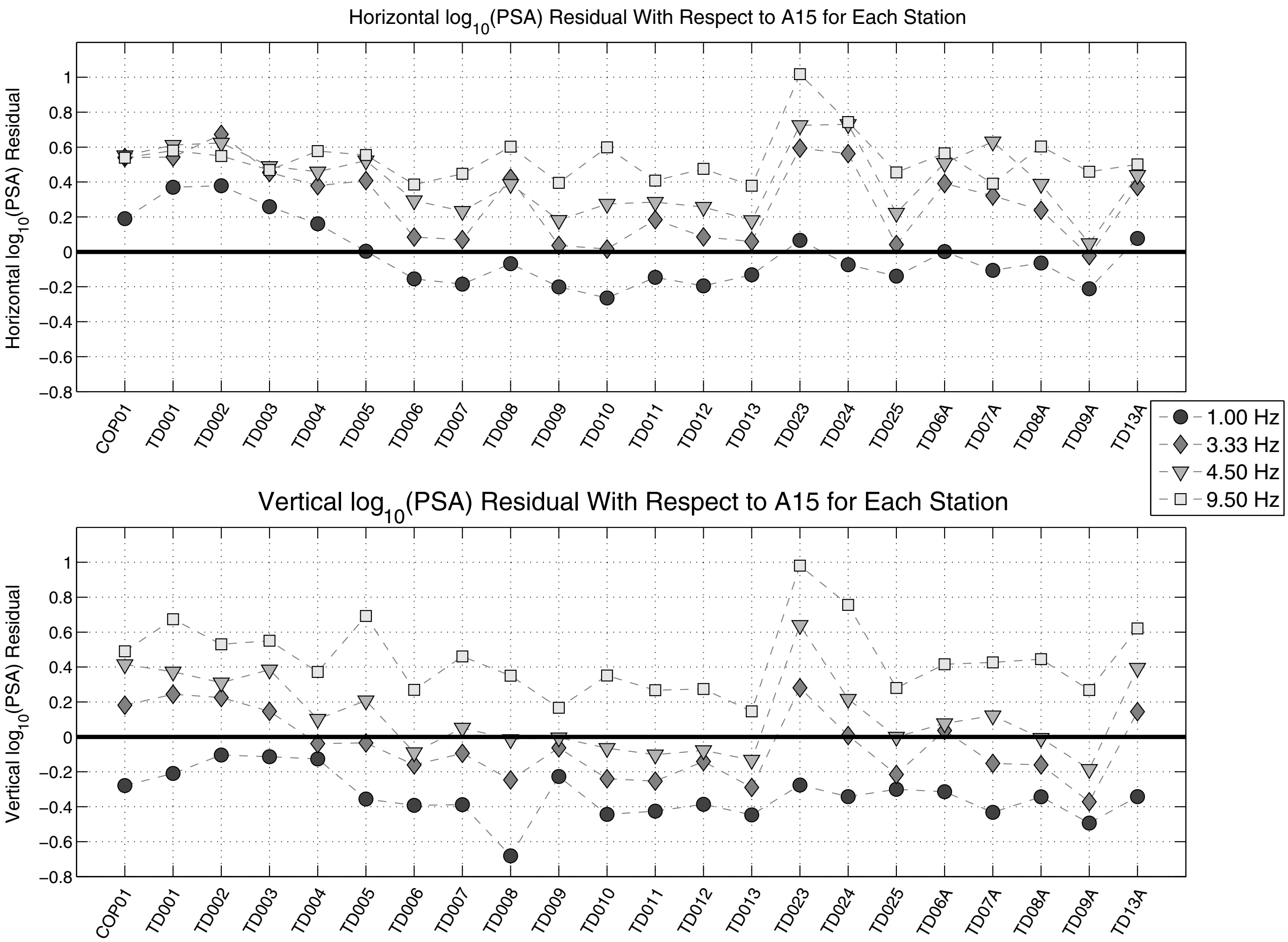

▲ **Figure 10.** The average station residuals for the vertical and horizontal components of selected frequencies, for events with **M** >2.6 (blasts excluded).

in this region. Ground-motion observations at close distances ($R < 50$ km) will be particularly valuable, as will a larger number of events. A larger number of events would facilitate the distinction between natural and induced events and illuminate any geographical effects related to the tectonic setting (location relative to the deformation front). This will provide a baseline for evaluating whether the ground-motion attributes of induced events differ significantly from those of natural earthquakes and whether these differences can be entirely attributed to focal depth effects.

CONCLUSIONS

This preliminary evaluation of ground motions in Alberta has determined the following:

1. The ground motions for small events in Alberta are generally consistent with those for similar-size events in California (as characterized by the AGY14 and A15 GMPEs) in terms of overall amplitude level and attenuation, but there are features in the residuals that require further investigation with additional ground-motion data.
2. The scaling characteristics of the Alberta events are generally consistent with expectations based on both empirical (Atkinson, 2015) and point-source simulation models (Yenier and Atkinson, 2015a).
3. There appears to be significant site response on the horizontal component in the 2–5 Hz frequency range, which is relatively consistent among stations, suggesting a common site response model for stations in western Alberta.

ACKNOWLEDGMENTS

This study was financially supported by the Natural Sciences and Engineering Research Council of Canada and TransAlta. The constructive comments of Justin Rubinstein, Jack Baker, and an anonymous referee are gratefully acknowledged.

REFERENCES

Anderson, J., and S. Hough (1984). A model for the shape of the Fourier amplitude spectrum of acceleration at high frequencies, *Bull. Seismol. Soc. Am.* **74,** no. 5, 1969–1993.

Assatourians, K., and G. Atkinson (2010). Database of processed time series and response spectra for Canada: An example application to study of the 2005 M_N 5.4 Riviere du Loup, Quebec earthquake, *Seismol. Res. Lett.* **81,** no. 6, 1013–1031.

Atkinson, G. M. (2015). Ground-motion prediction equation for small-to-moderate events at short hypocentral distances, with application to induced seismicity hazards, *Bull. Seismol. Soc. Am.* **105,** no. 2A, doi: 10.1785/0120140142.

Atkinson, G., W. Greig, and E. Yenier (2014). Estimation of moment magnitude (**M**) for small events (**M** < 4) on local networks, *Seismol. Res. Lett.* **85,** 1116–1124.

Baranova, V., A. Mustaqeem, and S. Bell (1999). A model for induced seismicity caused by hydrocarbon production in the western Canada sedimentary basin, *Can. J. Earth Sci.* **36,** 47–64.

Building Seismic Safety Council (2009). NEHRP Recommended Provisions for Seismic regulations for New Buildings and other Structures (FEMA 750), Federal Emergency Management Agency, Washington, D.C.

Farrugia, J., and G. Atkinson (2015). A preliminary evaluation of site amplification in Alberta, *Undergraduate Thesis*, Western University, London Ontario, Canada.

Fereidoni, A., and G. Atkinson (2015). Identifying quarry blast events in seismicity catalogs based on ground motion parameters, *Canadian Geophysical Union (CGU) Annual Meeting*, Montreal, Canada, 3–7 May 2015 (unpublished).

Ghofrani, H., and G. Atkinson (2014). Site condition evaluation using horizontal-to-vertical spectral ratios of earthquakes in the NGA-West2 and Japanese databases, *J. Soil Dyn. Earthq. Eng.* **67,** 30–43.

Gu, Y., A. Okeler, L. Shen, and S. Contenti (2011). The Canadian Rockies and Alberta Network (CRANE): New constraints on the Rockies and western Canada sedimentary basin, *Seismol. Res. Lett.* **82,** 575–588.

Hough, S. (2014). Shaking from injection-induced earthquakes in the central and eastern United States, *Bull. Seismol. Soc. Am.* **104,** 2619, doi: 10.1785/0120140099.

Lermo, J., and F. Chávez-García (1993). Site effect evaluation using spectral ratios with only one station, *Bull. Seismol. Soc. Am.* **84,** 1350–1364.

Nigam, N., and P. Jennings (1969). Calculation of response spectra from strong-motion earthquake records, *Bull. Seismol. Soc. Am.* **59,** no. 2, 909–922.

Pacific Earthquake Engineering Research Center (2014). *NGA-West2 Ground Motion Database*, http://peer.berkeley.edu/ngawest2/databases/ (last accessed May 2015).

Schultz, R., V. Stern, and Y. Gu (2014). An investigation of seismicity clustered near the Cordel field, west central Alberta, and its relation to a nearby disposal well, *J. Geophys. Res. Solid Earth* **119,** 3410–3423.

Schultz, R., V. Stern, M. Novakovic, G. Atkinson, and Y. Gu (2015). Hydraulic fracturing and the Crooked Lake sequences: Insights gleaned from regional seismic networks, published online 23 April 2015, *Geophys. Res. Lett.* doi: 10.1002/2015GL063455.

Stern, V., R. Schultz, and G. Jean (2011). Alberta Microseismicity Project, Phase 1: Site assessments for the ATSN semipermanent stations and the PSEIP Strachan temporary seismic array, Energy Resources Conservation Board, *ERCB/AGS Open-File Rept. 2011-15*, 75 pp.

Yenier, E., and G. Atkinson (2015a). An equivalent point-source model for stochastic simulation of earthquake ground motions in California, *Bull. Seismol. Soc. Am.* **105,** no. 3, doi: 10.1785/0120140254.

Yenier, E., and G. Atkinson (2015b). A regionally-adjustable generic GMPE based on stochastic point-source simulations, *Bull. Seismol. Soc. Am.* **105** (unpublished).

Yenier, E., and G. M. Atkinson (2014). Equivalent point-source modeling of moderate-to-large magnitude earthquakes and associated ground-motion saturation effects, *Bull. Seismol. Soc. Am.* **104,** 1458–1478.

Mark Novakovic
Gail M. Atkinson
Department of Earth Sciences
Western University
London, Ontario N6G 2V4
Canada
mnovako3@uwo.ca
gmatkinson@aol.com